1999 Roon Awards Competition Paper

Effect of Carbon Black on Adhesion to Plastics in Solventborne 2K Polyurethanes

Kalpana S. Katti and Marek W. Urban†—The University of Southern Mississippi*

These studies show that when the pigment volume content (PVC) of carbon black particles increases in polyurethanes (PUR), NCO consumption increases, and the extent of H–bonded C=O species near the film-substrate (F–S) interface is enhanced. During crosslinking, polyurea (PUA) is produced, and its concentration levels near the F–S interface are diminished for unpigmented coatings, whereas for the same system containing carbon black, the PUA formation is enhanced. Although the presence of carbon black particles at the F–S interface results in diminished adhesion of 2K PUR to acrylonitrile-butadiene-styrene (ABS), adhesion is also affected by the presence of OH and C=O functionalities on ABS, which are potential sites for H— bonding to PUR. Stronger hydrogen donor affinity of N–H functionalities in PUA as compared to the N–H groups on PUR leads to increased H–bonding in the presence of carbon black. Enhanced intermolecular H–bonding in PUR due to the presence of carbon black particles competes with the F–S interfacial H–bonding that promotes adhesion.

INTRODUCTION

Multi-component polymeric systems are often complex not only due to the nature of the organic phase and crosslinking reactions leading to film formation, but also due to the presence of other phases. For example, if an inorganic phase is dispersed in a thermosetting polymer system, individual components may not only become adsorbed on surfaces of inorganic particles before crosslinking, thus altering their proper stoichiometric levels, but an inorganic phase may stratify, leading to concentration gradients across the film thickness. Thus, multiphase systems are complex and this behavior is particularly pronounced for polyurethanes (PUR), which are typically formed by reactions of NCO and OH functionalities to form crosslinked networks.[1-3] Due to NCO reactivity, crosslinking reactions are sensitive to relative humidity (RH) and other environmental effects.[4-8] When carbon black particles[9,10] are added to PUR, a number of properties can be altered, and although previous studies on alkyds[11] and epoxies[12] provided some insights into inorganic/organic phase interactions and possible causes for stratification of pigment particles, the effect of pigmentation on adhesion has not been addressed. As a matter of fact, stratification processes in coatings and practical consequences associated with them have not been recognized until during last decade.[13-19] In an effort to elucidate the influence of carbon black in PURs on adhesion to plastics and to assess molecular level processes that govern coating-substrate interactions in the presence of carbon black particles, these studies focus on molecular level analysis of interfaces and their effect on adhesion in a PUR/acrylonitrile-butadiene-styrene (PUR/ABS) double layer system. Specifically, we will attempt to examine stratification processes in PUR and the effect of ABS surface morphology on PUR adhesion.

Presented at the 77th Annual Meeting of the Federation of Societies for Coatings Technology, on October 18-22, 1999, in Dallas, TX.

*School of Polymers and High Performance Materials , Shelby F. Thames Polymer Science Research Center, Hattiesburg, MS 39406.

†Author to whom all correspondence should be addressed.

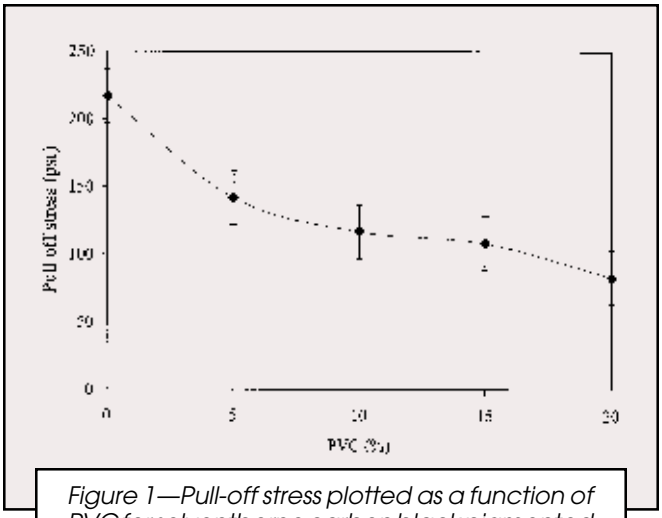

Figure 1—Pull-off stress plotted as a function of PVC for solventborne carbon black pigmented 2K PUR coating on ABS-CYCOLAC substrate.

EXPERIMENTAL

Sample Preparation

Hydroxyl-substituted polyacrylate (Desmophen A450A) and an aliphatic polyisocyanate, 1,6-hexamethylene diisocyanate (HDI) (Desmodur N3300) were obtained from Bayer Corp. Polyacrylate and 1,6-HDI crosslinker were mixed in a 1.1:1.0 molar ratios and stirred for two minutes. Carbon black powders with particle sizes of 14, 45, and 75 nm, obtained from Cabot Corp., were utilized in these studies, and PUR coatings were formulated at 0, 5, 10, 15, and 20% pigment volume content (PVC). Carbon black particles were added to polyacrylate, stirred for two minutes and allowed to stabilize for one hour. At this point 1,6-HDI was stirred with the mixture of polyacrylate and carbon black for two minutes. Such formulated films were coated on to polytetrafluoroethylene (PTFE) (PTFE Industries, Inc.) and acrylonitrile-butadiene-styrene (ABS) (GE Plastics) substrates, and allowed to crosslink for 90 hr under 75-80% RH conditions.

In an effort to alter the amount of H_2O adsorbed on carbon particle surfaces and replace it with D_2O (H_2O – D_2O exchange), carbon black particles were heated to 150°C in a vacuum oven for two hours, followed by mixing with D_2O and drying in a vacuum oven at 150°C for one hour prior to dispersing in polyacrylate under He atmosphere. Such a prepared dispersion was allowed to crosslink with 1,6 HDI under D_2O atmosphere at 75-80% RH for 72 hr.

Spectroscopic Measurements and Testing

Photoacoustic FTIR spectral measurements were performed using a Nicolet 850 Series II FTIR spectrometer equipped with a PA cell (MTEC 100, MTEC Inc). For step-scan (SS) PAS spectral acquisitions, a resolution of 8 cm^{-1} and modulation frequencies ranging from 25 to 1000 Hz were used. The variation of modulation frequency enabled measurements from depths ranging from approximately 7 to 50 μm for PUR and 7 to 43 μm for ABS. All sample spectra were ratioed against carbon black reference obtained in a pellet form from MTEC Inc. Attenuated total reflectance (ATR) Fourier transform infrared (FTIR) measurements were performed on a Nicolet 850 Series II FTIR instrument equipped with a Spectra Tech Inc. ATR cell. Depth profiling was achieved by varying the angle of incidence from 40° to 60° using a KRS5 crystal. The spectra were corrected for optical defects using Q-ATR[20] software. Data acquisition was obtained using Omnic ESP™ FTIR software (Nicolet Instrument Corp.) and spectral manipulations were performed using Grams32™ software (Galactic Industries Corp.). Deconvoluted spectra were generated from the best estimation of a maximum probability approach using physical information about spectral features and statistical knowledge of the number of overlapping

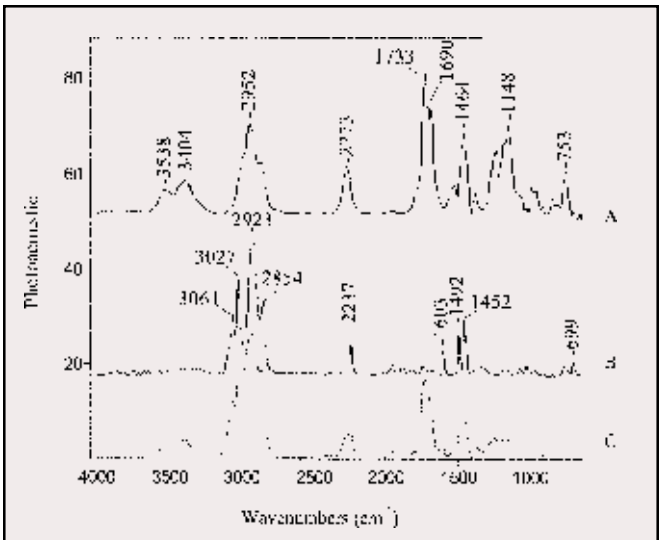

Figure 2—SS PAS spectra of PUR (A), ABS (B), and 5% PVC carbon black pigmented PUR on ABS (C).

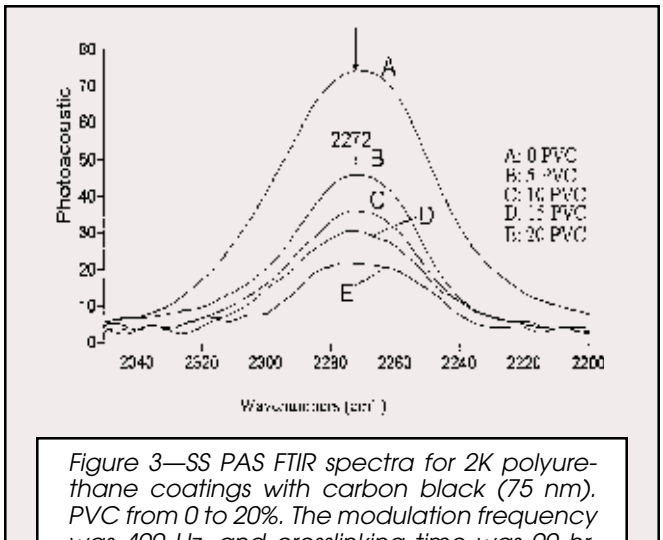

Figure 3—SS PAS FTIR spectra for 2K polyurethane coatings with carbon black (75 nm). PVC from 0 to 20%. The modulation frequency was 400 Hz, and crosslinking time was 90 hr. Relative humidity was 78%. Trace A: 0% PVC, Trace B: 5% PVC, Trace C: 10%, Trace D: 15% PVC, and Trace E: 20% PVC.

bands. SSRES™ (Galactic Industries Corp.) software is utilized for this purpose.

Adhesion tests were performed using Model 106 Elcometer (Elcometer Instruments Ltd., England), in which the stress required to pull off PUR from an ABS substrate was measured.

RESULTS AND DISCUSSION

As was indicated in the Introduction, the presence of carbon black in an organic phase may significantly affect numerous properties,[21,22] and adhesion to plastic substrates may be one of these properties. For that reason, pull-off stress required to remove PUR film attached to ABS as a function of PVC in PUR was measured. The results are shown in *Figure* 1, and as seen, a decrease of adhesion of 2K PUR to ABS is observed when PVC increases. This poses the first question as to what causes this behavior and, ultimately, what factors contribute to the diminished adhesion.

With these macroscopic observations in mind, we would like to understand the origin of this behavior. Although one would suspect that the carbon black content might result in an uneven distribution of pigment particles due to flow-related effects, at this point the origin of this behavior is only speculative. For that reason we utilized photoacoustic FTIR spectroscopy, as this method allows us to perform nondestructive determination of the chemical makeup at different surface depths.[23-24] However, before these attempts are made, the first step is to identify spectral features of PUR and ABS. *Figure* 2, Traces A, B, and C show PA FTIR spectra of PUR, ABS, and five percent PVC pigmented PUR on ABS, respectively, recorded using 50 Hz modulation frequency. While *Tables* 1 and 2 summarize tentative band assignments for 2K PUR and ABS, *Appendix* I describes the relevant formulas, and how depths of penetration can be estimated from the ATR and PA FTIR measurements. In the PUR spectrum (Trace A), the bands at 3538 and 3404 cm^{-1} are attributed to the OH and N—H stretching normal vibrations, and the bands at 2986, 2952, and 2863 cm^{-1} result from asymmetric —CH_3, and asymmetric/symmetric CH_2 stretching modes, respectively. The asymmetric CH_2 band at 2952 cm^{-1} is used for spectral normalization. The band at 2273 cm^{-1} is of a particular interest because this spectral feature is attributed to NCO out-of-phase vibrations of isocyanate. The 1700 cm^{-1} region of the spectrum shows strong bands due to free and H—bonded C=O stretching vibrations resulting from polyacrylate (1733 cm^{-1}), isocyanurate (1690 cm^{-1}), polyurethane (1733 cm^{-1}, 1712 cm^{-1}), and polyurea (1690 cm^{-1}, 1652 cm^{-1}, 1636 cm^{-1}).[25-27] With this background in mind, let us focus on the effect of carbon black particles on PUR

Table 1—Tentative Band Assignments for PUR System

	Wavenumber (cm^{-1})			
Band Assignment	**Acrylic Polyol**	**Isocyanurate**	**Polyurethane**	**Polyurea**
H—bond. OH str.	3543	—	3538	3538
H—bond N—H str.		—	3404	3404
ν_a CH_3	2999	—	2986	2988
ν_a CH_2	2952	2939	2952	2952
ν_s CH_3	2879	2862	2872	2872
NCO out-of-phase		2273	—	—
Free C=O str.	1731	1690	1733	1691, 1652
H—bond C=O str.	—		1712	1636
δ N—H & ν_a C—N	—	1511	1525	1525
δ CH_2	1451	1465	1463	1463
δ—C (CH_3)	1388	1376	1384	1384
δ N—H & vs C—N	—	1368	1367	1367
NCO in-phase	—	1338	—	—
(O=) C—O—C str.	1243	—	1243	1243
ν_a C–N–C str.	—	1189	1189	1189
(O=) C—O—C str.	1192	—	1170	1170
(O=) C—O–C str.	1150	—	1150	1150
ν C–N		1090		
n-butyl	1079	—	1068	1068
C—C skel. vib.		1033	—	—
C—C skel. vib.	990	—	990	990
C—C skel. vib.	967	—	967	967
ν_s C—N—C	—	846	845	845
C—N skel. str.	—	768	767	767
CH_2 in-phase rock	751	730	753	753

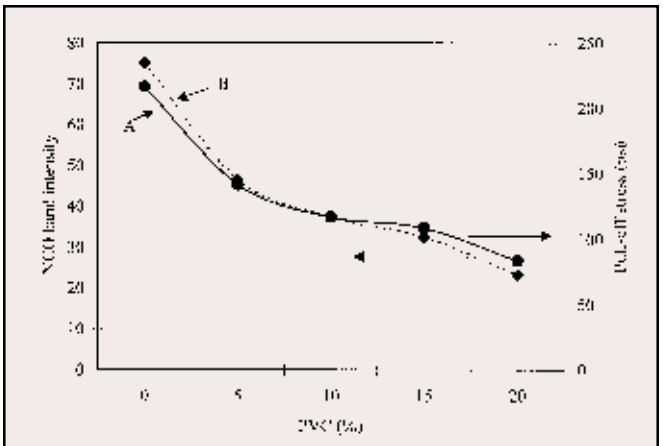

Figure 4—Plot of NCO band intensity (curve A) and pull-off stress (curve B) vs. PVC.

Table 2—Tentative Band Assignments for ABS

	Wavenumber (cm^{-1})		
Band Assignment	**Acrylonitrile**	**Butadiene**	**Styrene**
Aromatic C–H stretching			3061
Aliphatic C–H stretching	2923	2854	
—C≡N stretching	2237		
Aromatic C—C		1452	1492
Overtones-monosubstituted	—	—	—
benzene	—	—	2000-1667
C=C stretching	—	1603	—
CH_2 rocking—			
1, 4 Polybutadiene	—	965	—
CH_2 rocking—			
1,2 Polybutadiene	—	912	—
C—H aromatic			
Out-of-plane deformation	—	—	699

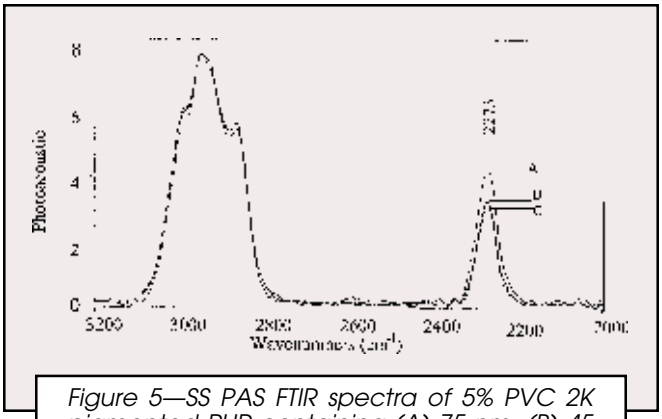

Figure 5—SS PAS FTIR spectra of 5% PVC 2K pigmented PUR containing (A) 75 nm, (B) 45 nm, and (C) 14 nm carbon particle sizes.

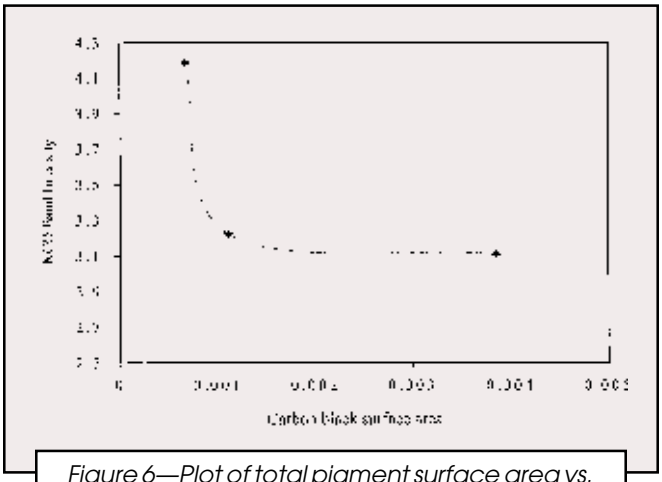

Figure 6—Plot of total pigment surface area vs. intensity of isocyanate band for carbon pigmented PU coatings.

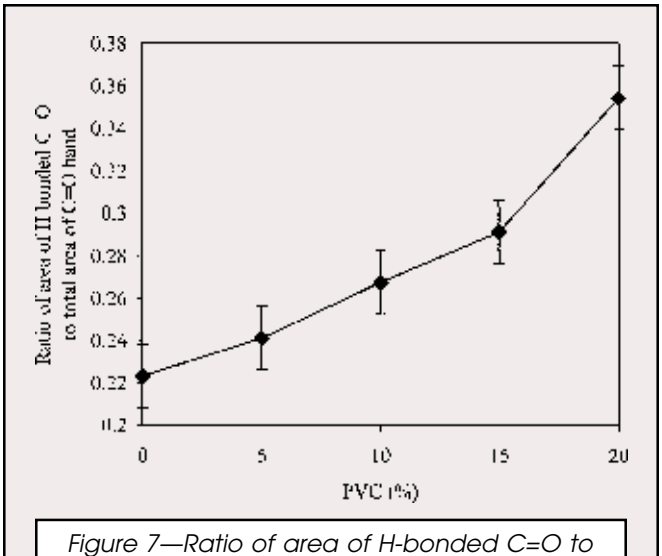

Figure 7—Ratio of area of H-bonded C=O to area of total C=O for 0 to 20% PVC 75 nm sized carbon pigmented PUR on ABS.

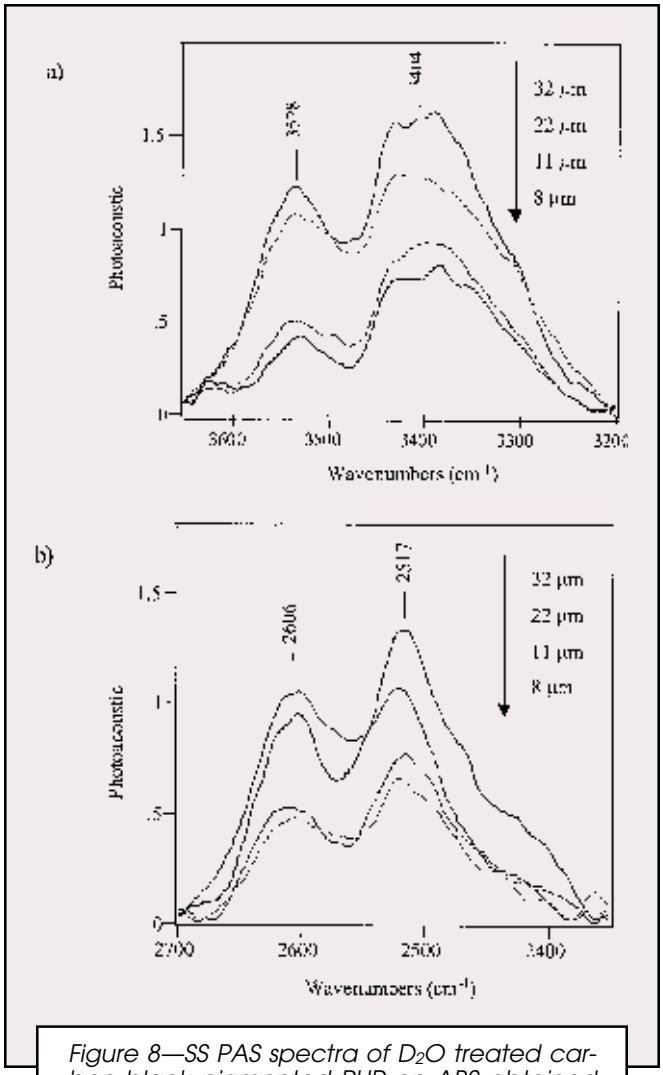

Figure 8—SS PAS spectra of D_2O treated carbon black pigmented PUR on ABS obtained from depths of 32 μm, 22 μm, 11 μm, and 8 μm from surface in the (A) O-H and (B) O-D spectral regions.

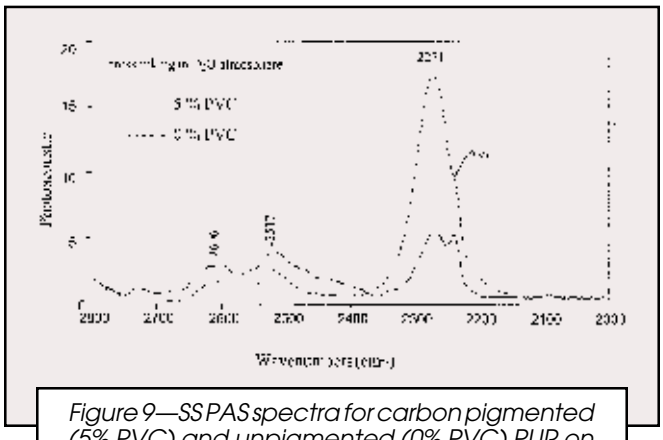

Figure 9—SS PAS spectra for carbon pigmented (5% PVC) and unpigmented (0% PVC) PUR on ABS near O-D band at 50 Hz modulation frequency.

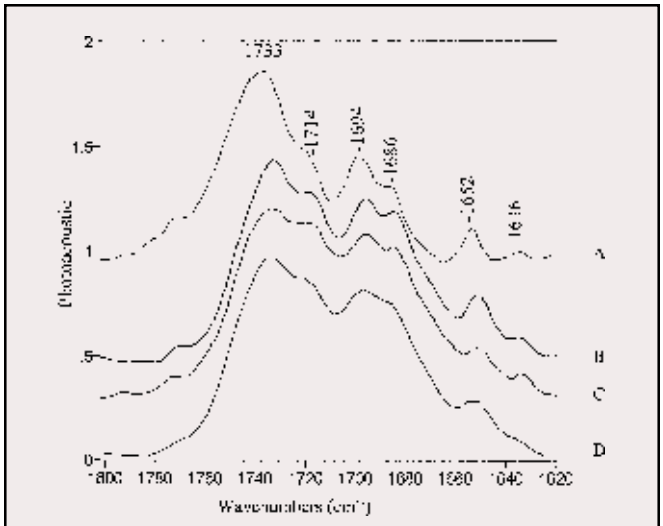

Figure 10—Depth profiling of 5% PVC carbon pigmented PUR on ABS. SS PAS from 7.2 μm (A), 11.4 μm (B), 16.1 μm (C), and 32.2 μm (D).

crosslinking and the effect of ABS surface morphology on adhesion.

Effect of Carbon Black on PUR Crosslinking

First, let us examine how PVC will affect the NCO functionality changes. *Figure* 3, Traces A-E, show SS PAS spectra in the 2340-2200 cm^{-1} region of 2K PUR containing 0-20% PVC recorded at 400 Hz which corresponds to about 11 μm penetration depth from the F-A interface. As seen, an increase of the NCO consumption with addition of carbon black is observed. *Figure* 4, Curve A, plots the same NCO band intensity changes as a function of PVC, and in an effort to illustrate that the NCO consumption at a given reaction time parallels adhesion decrease as a function of PVC, the data from *Figure* 1 was re-plotted as Curve B.

Although it is quite apparent that the consumption of NCO as a function of PVC and adhesion changes parallel each other, the origin of this behavior is not clear. Because particle size may affect the extent of NCO consumption, the next question to be addressed is the effect of carbon black particle size on the NCO consumption. For that reason we analyzed the same PUR system which contained 14, 45, and 75 nm carbon black particle sizes at a five percent PVC level. SS PAS spectra of five percent PVC carbon pigmented 2K PUR are shown in *Figure* 5. As seen, the NCO band intensity decreases as the particle size decreases. Since the pigment particle size increase facilitates lesser surface area, let us estimate the total available surface area (S) of pigment particles. This is given by:

$$S = 4\pi r_i^2 (N) \qquad (1)$$

where: r_i is the pigment particle radius and N is the total number of particles dispersed in an organic phase. Since PVC can be expressed in terms of the ratio of the volume occupied by N particles to the total volume of a crosslinked system V_T,

$$PVC = \frac{4/3\pi r_i^3 N}{V_T} \qquad (2)$$

for a constant coatings thickness, and substituting N, the total surface area available for potential absorption of organic phase can be expressed as

$$S = \frac{1}{r_i} V_T PVC \qquad (3)$$

Using this relationship, a plot of the NCO intensity changes as a function of surface area for a constant coatings thickness at five percent PVC was constructed. This is shown in *Figure* 6, where a decrease of the NCO consumption for normalized pigment particle surface area is observed, indicating that the reduced surface area of carbon black particles leads to reduced consumption of the NCO groups in PUR; thus, suggesting that the surface area of carbon black particles plays a role in PUR crosslinking reactions.

Let us go back to *Figure* 2, Trace C, which is the SS PAS spectrum of pigmented PUR on ABS. The 1600-1800 cm^{-1} region of the spectrum exhibits characteristic bands resulting from H—bonded and 'free' C=O groups at 1733 and 1690 cm^{-1}. Since C=O groups exhibit high affinity towards H—bonding, let us examine if there are changes in H—bonded C=O groups with respect to the total C=O content as a function of PVC. SS PAS data were obtained at approximately 32 μm from the surface. The appearance of aromatic C—H stretching bands from ABS in the PAS spectra indicated that the spectra were obtained from a region near the F—S interface. *Figure* 7 illustrates H— bonded C=O at 1712 cm^{-1} area ratioed to the total C=O band area of the 1733 and 1712 cm^{-1} bands. These data indicate that the extent of H-bonded C=O groups increases with PVC. Thus, these experiments

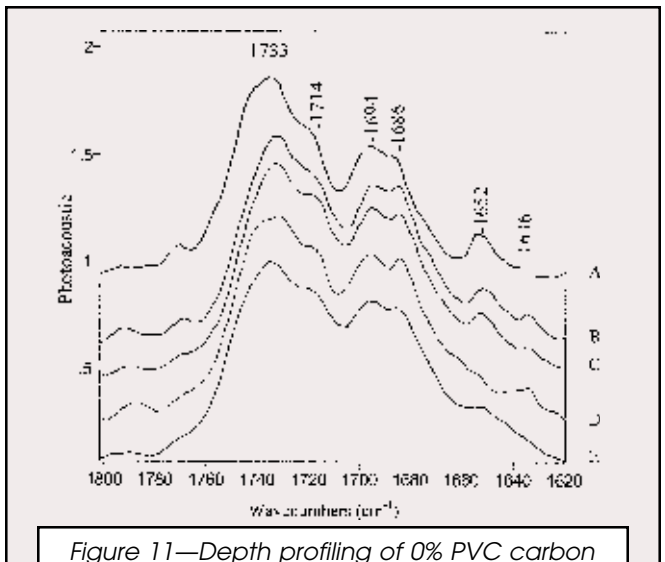

Figure 11—Depth profiling of 0% PVC carbon pigmented PUR on ABS. SS PAS from 7.2 μm (A), 8.2 μm (B), 11.4 μm (C), 16.1 μm (D), and 32.2 μm (E).

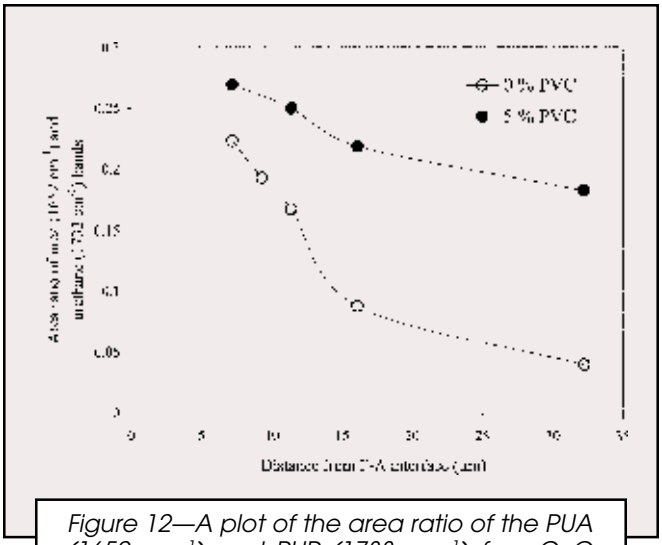

Figure 12—A plot of the area ratio of the PUA (1652 cm^{-1}) and PUR (1733 cm^{-1}) free C=O bands vs. distance from the F–A interface for unpigmented and 5% PVC carbon pigmented PUR coatings on ABS.

ing the formulation process carbon black particles were first added to polyacrylate, there is still a possibility that if OH groups are adsorbed to the surface, reactions such as those shown in *Scheme* 1 may occur, especially since carbon black surface adsorbs water which may react with isocyanate to yield amine and CO_2.[4]

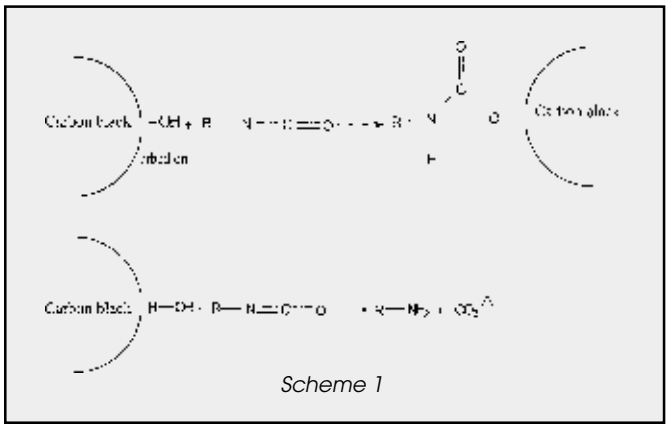

Scheme 1

show that, with addition of carbon black, there is an enhanced intermolecular H— bonding in PUR near the F—S interface. Furthermore, higher NCO consumption and increased inter-molecular H—bonding in PUR with addition of carbon black particles suggest the presence of reactive sites on carbon black surfaces. Although during the formulation process carbon black particles were first added to polyacrylate, there is still a possibility that if OH groups are adsorbed to the surface, reactions such as those shown in *Scheme* 1 may occur, especially since carbon black surface adsorbs water which may react with isocyanate to yield amine and CO_2.[4]

In order to examine if surfaces of carbon black particles affect the NCO consumption, and ultimately PUR adhesion, H_2O and OH groups adsorbed on carbon black particles were replaced with D_2O/OD. Such prepared particles with a 75 nm particle size were added to polyacrylate to obtain PUR with five percent PVC, and allowed to crosslink on ABS, followed by spectroscopic surface depth profiling from 7-32 μm and adhesion measurements. *Figure* 8 illustrates SS PAS spectra in the OH (a) and OD (b) stretching regions. It is apparent that the OH intensity at 3404 cm^{-1} decreases at shallower depths, indicating reduced concentrations of the OH species near the F—A surface, and their increase is observed when approaching the F—S interface. These results are in agreement with the previous studies on unpigmented PUR.[5] As shown in *Figure* 8b, reduced intensity of the OD band at 2517 cm^{-1} is observed near the F—A interface, and increases when approaching the F—S interface. Thus, behavior of the OD band is similar to its OH counterpart, which also increases closer to the F—S interface. Although one would like to utilize these experimental data and differentiate between surface and other OH containing enti-

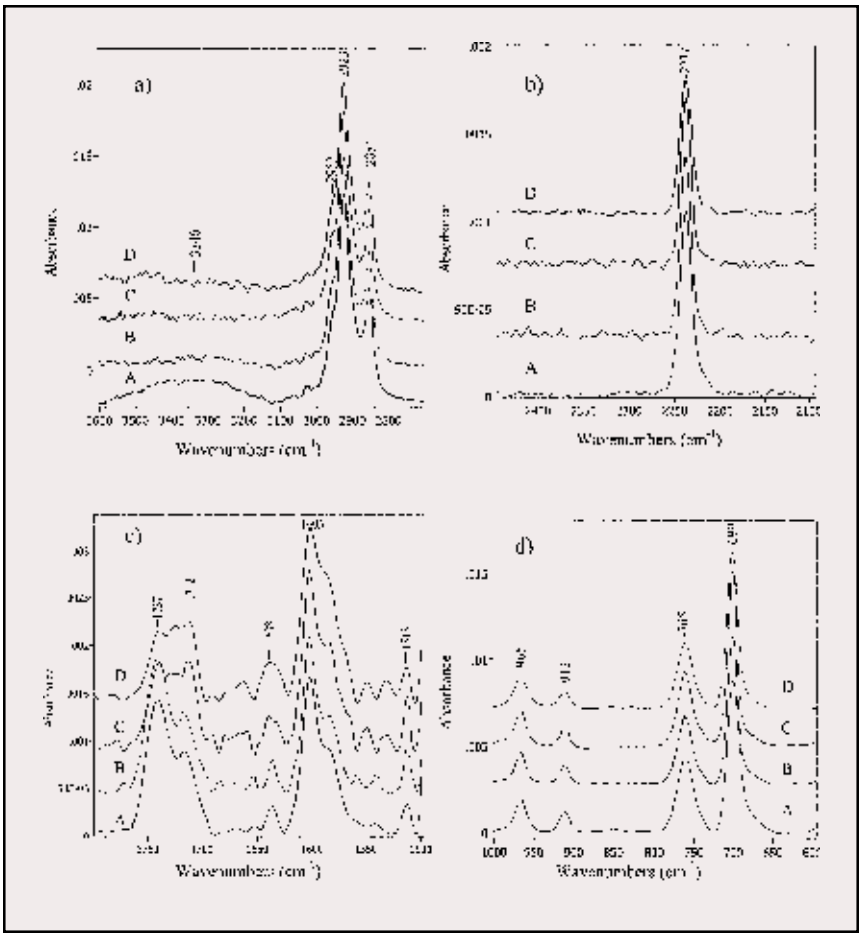

Figure 13—ATR FTIR spectra of ABS in the 2700-3600 cm^{-1} (A), 2100-3150 cm^{-1} (B), 1500-1800 cm^{-1} (C), and 600-1000 cm^{-1} (D) regions. Traces A-D are obtained from depths of penetration 0.65, 0.74, 0.88, and 1.2 μm at 1737 cm^{-1}.

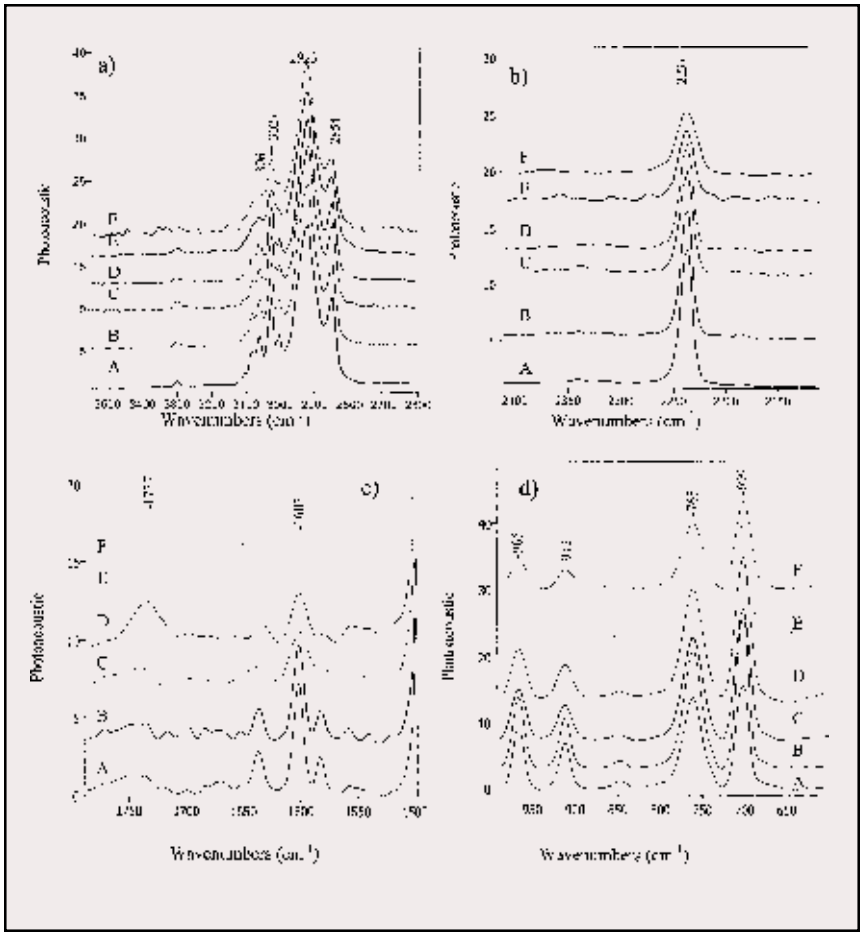

Figure 14—Linear PAS FTIR spectra of ABS in the 2600-3500 cm^{-1} (A), 2100-3150 cm^{-1} (B), 1500-1800 cm^{-1} (C), and 600-1000 cm^{-1} (D) regions. Traces A-F are obtained for mirror velocities 0.16 cm/s to 1.27 cm/s corresponding to depths of penetration 13.12 µm (A), 9.27 µm (B), 7.57 µm (C), 6.56 µm (D), 5.35 µm (E), and 4.72 µm (F) at 1737 cm^{-1}.

ties, it is well known that the proton transfer between oxygen and nitrogen containing compounds may be very fast, and upon mixing of OD-containing carbon black and polyol, the exchange may occur immediately.

SS PAS spectra of five percent PVC specimen and unpigmented PUR on ABS near the OD band from a 32 µm depth are shown in *Figure* 9. A decrease of the NCO band intensity at 2271 cm^{-1} results from the addition of carbon black as observed before, and an increase of the OD band intensity for pigmented PUR is observed, suggesting the presence of the OD groups on the surface of carbon black particles. Pull-off tests also showed no adhesion changes for the pull-off adhesion values between coatings formulated with D_2O labeled and natural abundant carbon black particles. Thus, the presence of OH or OD functionalities on carbon black surfaces affects adhesion between PUR and ABS to the same degree.

While the presence of OH/H_2O functionalities on the surface of carbon black particles justifies the increased consumption of NCO groups in pigmented coatings, previous studies[7] have shown the increased polyurea (PUA) formation in the presence of an excess of OH/H_2O species. In order to evaluate if indeed OH surface functionalities of pigment particles have a similar effect, depth profiling experiments using SS PAS were performed on zero and five percent PVC PUR coatings formulated with 75 nm carbon particles and coated on ABS. Changing modulation frequency allows us to perform depth profiling from about 7.2 to 32.2 µm. SS PAS spectra at 7.2 to 32.2 µm for zero percent PVC PUR coatings on ABS are shown in *Figure* 10, Traces A-D and *Figure* 11, Traces A-E for zero percent PVC. The spectra were normalized with respect to the 1733 cm^{-1} band and since the 1652 and 1733 cm^{-1} band area ratio determines relative amounts of PUA and PUR, it was plotted as function of film thickness. This is shown in *Figure* 12. As seen, the intensity of the 1652 cm^{-1} band, attributed to free C=O stretching vibrations of PUA decreases while approaching the F-S interface for both pigmented and unpigmented coatings. However, for pigmented PUR the intensity of the 1652 cm^{-1} band is enhanced near the F-S interface, indicating that for pigmented PUR, there is a higher PUA content near the F-S interface. Thus, the presence of carbon black indeed affects crosslinking reactions, in particular near the F-S interface.

Although up to this point our primary focus was on the effect of carbon black, substrate surface morphology may also affect adhesion. Thus, stratification within top surface layers of ABS may also affect adhesion to PUR. This phenomenon, which is often related to thermal history, was particularly explored for thermoplastic olefins (TPO).[28-33] For that reason, the relationship between surface properties of ABS and adhesion will be examined.

ABS Surface Morphology

In order to determine if surface morphology of ABS has an effect on adhesion, we utilized ATR FTIR, continuous, and SS PA FTIR spectroscopies. While *Appendix* 1 provides estimated penetration depths of each method, *Figures* 13-15 illustrate ATR, continuous PAS and SS-PAS spectra for ABS specimens and the tentative band assignments for ABS are shown in *Table* 2. *Figure* 13 shows the presence of a broad band in the 3000-3600 cm^{-1} region attributed to surface hydroxyl groups at 0.63 µm from the F-A interface. The presence of C=O groups is also marked at 0.65 µm, as seen by the enhanced intensity of the 1737 cm^{-1} band. At the same time concentration levels of the acrylonitrile component of ABS are diminished while going from 0.50 to 0.93 µm, which is demonstrated by the reduced intensity of the 2237 cm^{-1} band and no appreciable changes of the bands due to

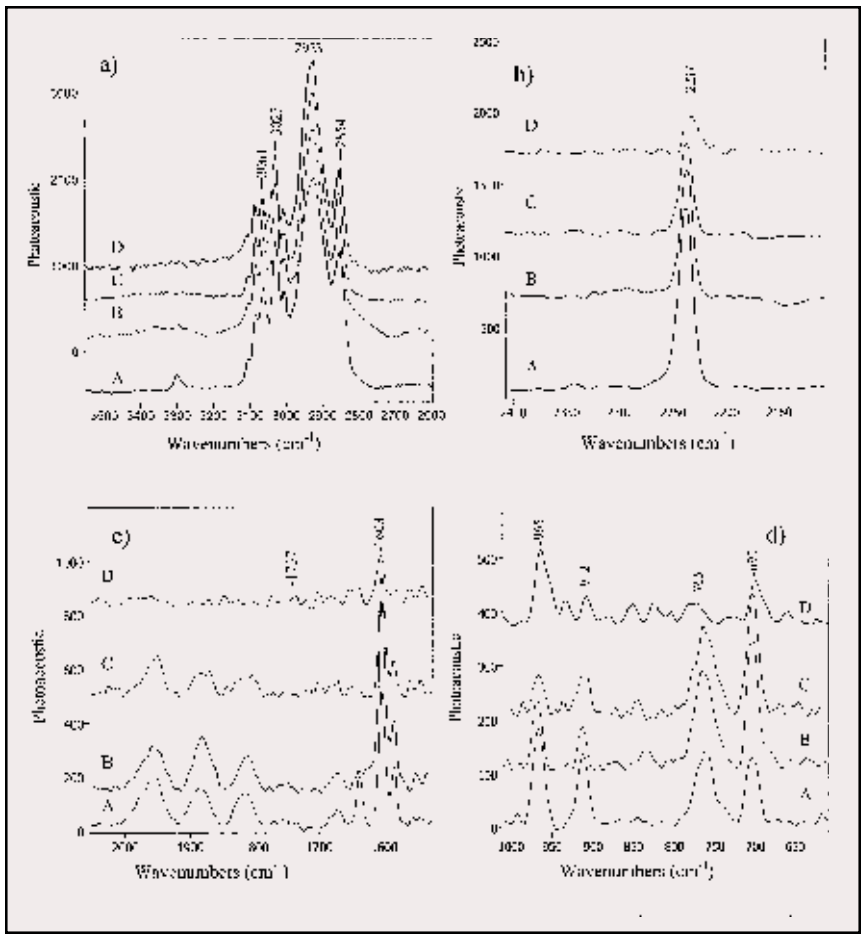

Figure 15—SS PAS FTIR spectra of ABS in the 2600-3500 cm^{-1} (A), 2100-3150 cm^{-1} (B), 1500-1800 cm^{-1} (C), and 600-1000 cm^{-1} (D) regions. Traces A-D are obtained for modulation frequencies 50 to 800 Hz corresponding to depths of penetration 30.76 μm (A), 15.38 μm (B), 10.87 μm (C), and 7.69 μm (D).

polybutadiene are detected from 1.17 to 2.16 μm. As shown in *Figure* 13a, aliphatic C—H stretching bands at 2854 cm^{-1}, 2923 cm^{-1}, and 2952 cm^{-1} are detected in Traces A-D, whereas aromatic C—H stretching bands (3027 cm^{-1} and 3061 cm^{-1}) are absent. Since C—H stretching bands due to aromatic groups are absent at 0-0.63 μm depth, styrene content is diminished within this distance from the surface.

While ATR FTIR experiments allow us to perform depth profiling from 0-3 μm, and provide evidence for ABS surface stratification, greater depths from the ABS surface can be probed using continuous PAS, which is accomplished by varying mirror velocity in the Michelson interferometer. *Figures* 14a-d, Traces A-F, show linear PAS FTIR spectra of ABS recorded at 0.16 cm/s to 1.24 cm/s mirror velocities in the 2600-3500, 2100-3150, 1500-1800, and 600-1000 cm^{-1} regions. These values correspond to approximate depths of 3.3 to 9.5 μm in the C—H stretching band region. The stratification of components from approximately 3 to 20 μm appears to be as follows: this region is marked by enhanced intensity of the C=O bands and decrease of the styrene bands as seen by the reduced intensities of the bands at 3027, 3061, and 1603 cm^{-1}. The concentration of acrylonitrile is also diminished in this region as reduced intensity of the —C≡N band at 2237 cm^{-1} is observed. Reduced intensities of the bands at 965 and 912 cm^{-1} suggest a reduced concentration of butadiene with depth from 6.2 to 17.6 μm and no OH functionalities are detected at this depth.

SS PAS offers a constant depth of penetration for all wavenumbers and at low modulation frequencies is capable of probing deeper. *Figure* 15a-d illustrates SS PAS FTIR spectra in the 2600-3500, 2100-3150, 1500-1800, and 600-1000 cm^{-1} regions. In these spectra, Traces A-D are obtained from 30.8, 15.4, 10.9, and 7.7 μm depths from the surface of ABS. This region shows an enhanced intensity of acrylonitrile when going deeper, as seen from the —C≡N stretching vibration at 2237 cm^{-1}. Higher concentration of styrene from 7.7 to 15.4 μm present in this region is evident by the presence of aromatic C—H stretching bands at 3027 and 3061 cm^{-1} and the 1603 cm^{-1} band that is accompanied by a reduced concentration of polybutadiene at these depth levels.

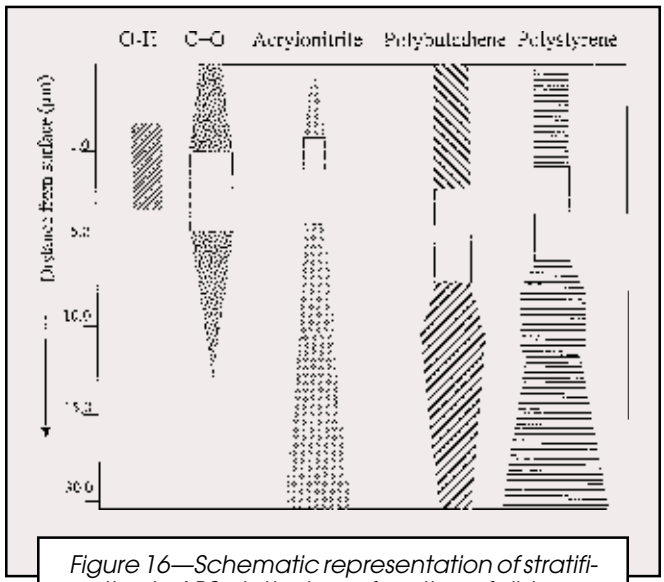

Figure 16—Schematic representation of stratification in ABS plotted as a function of distance from the surface. Relative concentrations of each component are porportional to the width of the bands.

Based on the previous experiments, a schematic diagram showing a stratification profile of ABS was constructed and is shown in *Figure* 16. It appears that there are three distinct regions near the ABS surface. From 0 to 4 μm, there are OH and C=O groups and increased concentration levels of acrylonitrile. This region also exhibits a constant concentration of polybutadiene and styrene. From 4 to 12 μm, there is an absence of the OH groups and decreased concentration of the C=O groups. While polybutadiene content increases, polystyrene also shows increased concentrations up to about 8 μm from the surface and its concentration levels up to 12 μm from the surface. From 12 to 30 μm there is a pronounced presence of acrylonitrile, butadiene, and styrene, but acrylonitrile and styrene contents increase when going deeper, whereas polybutadiene content decreases.

At this point it is appropriate to combine the PUR and ABS stratification profiles and relate them to adhesion and the carbon black PVC. As we recall, the presence of OH functional groups on carbon black competes with the formation of PUR. In essence, a higher PUA content is present closer to the F-S interface in carbon pigmented coatings and H-bonded interactions between C=O on PUR and N—H on PUA appear to be stronger than that between C=O and N—H groups on PUR because PUA are stronger hydrogen bond donors.[34] Due to competing reactions and higher affinity of the PUR/PUA interactions, H-bonding interactions of PUR with OH and C=O groups on the ABS surface cannot occur. This is schematically illustrated in *Figure* 17. Thus, the presence of carbon black reduces the coating-substrate H—bonding interactions by enhancing H—bonding interactions near the F—S interface of PUR, which ultimately leads to decrease of adhesion between PUR and ABS.

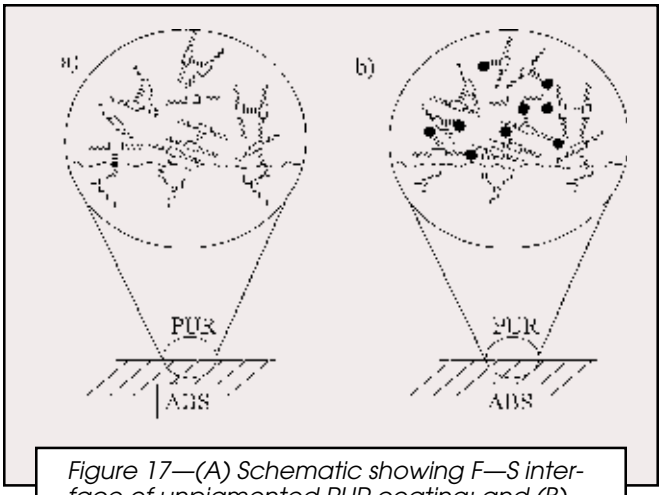

Figure 17—(A) Schematic showing F—S interface of unpigmented PUR coating; and (B) Schematic showing F—S interface of carbon pigmented coating. ▭ : PUR, ✹ carbon particle with urea formation on surface. ⁞⁞⁞⁞ H—bonding.

CONCLUSIONS

Adhesion between 2K PUR and ABS substrate is significantly reduced with the addition of carbon pigment. Increased PVC further reduces adhesion to ABS, and increases the extent of inter-molecular H—bonding in PUR coatings near the F—S interface. The presence of OH/H_2O functionalities particles are observed on the surface of carbon black which can effectively influence adhesion. In addition, an accelerated consumption of NCO and an increased PUA formation near the F-S interface is detected in pigmented PUR, which results from the presence of OH/H_2O functional groups on the pigment surfaces. Since the N-H groups on PUA have a larger acidic character as compared to the N—H groups on PUR, an enhanced PUA formation near F—S interface leads to increased H—bonding near the F—S interface. Surface stratification of ABS also affects adhesion and the presence of H—bonding species on ABS does not necessarily promote adhesion for pigmented PUR because increased inter-molecular H-bonding within pigmented PUR competes with the substrate functional groups.

ACKNOWLEDGEMENTS

The authors are thankful to the National Science Foundation Industry/University Cooperative Research Center in Coatings for the financial support of these studies, and Jim McGinness and Kevin Riggs of Red Spot Paint Co. for exploring these studies and useful discussions.

References

(1) Woods, G., *The ICI Polyurethane Book*, Second Edition, John Wiley & Sons, 1990.
(2) Oertel, G. (Ed.), *Polyurethane Handbook*, Second Edition, Hanser, New York, 1996.
(3) Urban, M.W., *Laboratory Handbook of Organic Coatings*, Global Press, Chicago, 1997.
(4) Kaminski, A.M. and Urban, M.W., *Polym. Mater. Sci. Eng.*, *74*, 220 (1996).
(5) Kaminski, A.M. and Urban, M.W., "Interfacial Studies of Crosslinked Polyurethanes: Part I. Quantitative and Structural Aspects of Crosslinking Near Film-Air and Film Substrate Interfaces in Solventborne Polyurethanes," JOURNAL OF COATINGS TECHNOLOGY, *69*, No. 872, 55 (1997).
(6) Kaminski, A.M. and Urban, M.W., "Interfacial Studies of Crosslinked Urethanes: Part II. The Effect of Humidity on Waterborne Polyurethanes; A Spectroscopic Study," JOURNAL OF COATINGS TECHNOLOGY, *69*, No. 873, 113 (1997).
(7) Urban, M.W., Allison, C.L., Finch, C.C., and Tatro, B.A., "Interfacial Studies of Crosslinked Urethanes: Part III. Structure-Property Relationships in Polyester Waterborne Polyurethanes," JOURNAL OF COATINGS TECHNOLOGY, *71*, No. 888, 75 (1999).
(8) Han, Q. and Urban, M.W., *J. Appl. Polym. Sci.*, in press.
(9) Stevenson, W.T.K. and Garton, A., *J. Mater. Sci. Lett.*, *6*, 580-582 (1987).
(10) Baikov, M.V., Ponyavina, A.N., Prishivalko, A.P., Sviridov, V.V., and Sil'vanovich, N.I., *J. Appl. Spect.*, *63*,[3], 297 (1996).
(11) Urban, M.W. and Salazar-Rojas, E.M., *J. Polym. Sci. Part A: Polym. Chem.*, *28*, 1593-1613 (1990).
(12) He, M., Urban, M.W., and Bauer, R.S., *J. Appl. Polym. Sci.*, *49*, 345, 1993.
(13) Urban, M.W. and Evanson, K.W., *Polym. Commun.*, *31*, 279, 1990.
(14) Evanson, K.W., and Urban, M.W., *J. Appl. Polym. Sci., 42(8)*, 2287 (1991).

(15) Hirayama, T., and Urban, M.W., *Prog. Org. Coat., 20*, 81 (1992).
(16) Thorstenson, T.A., Tebelius, L.K., and Urban, M.W., *J. Appl. Polym.Sci., 49*, 103 (1993).
(17) Niu, B.J. and Urban, M.W., *J. Appl. Polym.Sci., 56*, 377 (1995).
(18) Martin, L.R. and Urban, M.W., *J. Appl. Polym.Sci., Vol. 62*, 1893 (1996).
(19) Allison, C.L, Urban, M.W., Johnoson, G.L., and DiStefano, F., *Appl. Spectrosc., 53*, 1520, 1999.
(20) Urban, M.W., *Attenuated Total Reflectance Spectroscopy of Polymers; Theory and Practice,* American Chemical Society, 1996.
(21) Orel, Z.C., *Proc. SPIE*, *2531*, 296 (1995).
(22) Lakdawala, K. and Salovey, R., *Polym. Eng. Sci.*, *27*, 1035 (1987).
(23) Rosencwaig, A., *Photoacoustics and Photoacoustic Spectroscopy*, Robert E. Krieger Publishing Company, Malabar, Florida, 1980.
(24) Urban, M.W., *Vibrational Spectroscopy of Molecules and Macromolecules on Surfaces*, John Wiley & Sons, Inc., New York, 1993.
(25) Sun, H., *Macromolecules*, *26*, 5924-5936 (1993).
(26) Coleman, M.M., Lee, K.H., Skrovanek, D.J., and Painter, P.C., *Macromolecules*, *19*, 2149 (1986).
(27) Coleman, M.M., Skrovnak, D.J., Hu, Jianbin, and Painter, P.C., *Macromolecules*, *21*, 59-65 (1988).
(28) Ryntz, R.A., *Adhesion to Plastics; Molding and Paintability,* Global Press, Chicago, 1998.
(29) Stegge, J. and Urban, M.W., *Polymer*, submitted for publication.
(30) Pennington, B., Ryntz, R.M., and Urban, M.W., *Polymer*, *40*, 4795 (1999).
(31) Kiland, B. and Urban., M.W., *Polymer*, in press.
(32) Ryntz, R.A., *Prog. Org. Coat.*, *27*, 241 (1996).
(33) Carter III, R.O. and McCallum, J.B., *Polymer Degradation and Stability*, *45*, 1 (1994).
(34) Luo, N., Wang, D.N., and Ying, S.K., *Polymer*, *37*, 3045 (1996).

Appendix 1

Depth Profiling in ATR, Continuous, and SS FTIR PAS Experiments

Depth Probed in ABS	Parameters	Method
0.34 - 2.98 μm at 3340 - 699 cm^{-1} incidence angle: 45°-60°	λ_0: wavelenth of light in the internal reflection crystal θ: angle of incidence n_{21}: refractive index ratio of the sample (n_2) and crystal (n_1).	**Attenuated Total Reflectance** $d_p = \frac{\lambda_0}{2\pi n_1\left(\sin^2\theta - n_{21}^2\right)^{1/2}}$ Depth of penetration is wavenumber dependent and is achieved by varying the angle of incidence.[17] QATR[13] program is used to correct the ATR data for optical corrections. Estimated depths of penetration are accurate.
3.34 - 20.68 μm at 3340 - 699 cm^{-1} mirror velocity: 0.16 - 1.27 cm/s	V: velocity of moving mirror ν: wavenumber α: thermal diffusivity α=k/ρC k: thermal conductivity ρ: density C: specific heat	**Continuous Photoacoustic Spectroscopy** $\mu_{th} = \left[\frac{\alpha}{\pi\sqrt{\nu}}\right]^{1/2}$ Depth profiling is achieved by varying the mirror velocity of the moving mirror.[16,17] Depth of penetration is wavenumber dependent. Estimated depths of penetration are approximate.
6.87 - 43.49 μm modulation frequency: 25 - 1000 Hz	ω: modulation frequency of incident radiation α: thermal diffusivity α=k/ρC k: thermal conductivity ρ: density C: specific heat	**Step-Scan Photoacoustic Spectroscopy** $\mu_{th} = \left[\frac{2\alpha}{\omega}\right]^{1/2}$ Depth profiling is achieved by varying the modulation frequency of the incident radiation.[16,17] A constant depth of penetration is achieved for all wavenumbers. Estimated depths of penetration are approximate.